

# DETERMINATION OF PHYSICAL PARAMETERS OF PELLETTED RICE SEEDS AND CALIBRATION OF DISCRETE ELEMENT SIMULATION PARAMETERS

## 丸粒化水稻种子物性参数测定与离散元仿真参数标定

Qianshu MA<sup>1)</sup>, Tongjie LI<sup>1)</sup>, Donghan XU<sup>1)</sup>, Qingqing WANG<sup>\*1)</sup>

<sup>1)</sup>Anhui University of Science and Technology, Bengbu, China

<sup>\*)</sup> Corresponding author E-mail: qqwang@ahstu.edu.cn; Tel: +86-13195519097

DOI: <https://doi.org/10.35633/inmateh-75-42>

**Keywords:** pelleted rice seeds; seed mechanics; simulation experiment; parameter calibration

### ABSTRACT

The calibration of parameters for pelleted rice seeds (PR) is crucial for enhancing research on PR-related machinery and for executing high-speed precision hole sowing with unmanned aerial vehicles. This paper focuses on determining the fundamental physical and contact parameters of PR. A series of tests were conducted, including the Plackett-Burman test, the steepest ascent test, and the Box-Behnken test, using the stacking angle as the primary variable. These tests led to the identification of optimal combinations of simulation parameters. Specifically, the coefficients of rolling friction for the PR-PLA plate and PR-PR were measured at 0.137, while the coefficient of static friction for the PR-PLA plate was 0.336. This study provides a reference for calibrating simulation parameters of pelleted seeds and research on high-speed precision seeding.

### 摘要

丸粒化水稻种子的参数标定, 可以为丸粒化水稻相关机械的研究及无人机的高速精量穴播提供指导。本文以丸粒化的水稻为对象, 对其基本物性参数和接触参数开展测定。以堆积角为试验值进行 Plackett-Burman 试验、最陡爬坡试验和 Box-Behnken 试验, 获得最佳仿真参数组合 (丸粒化水稻种子-PLA 板滚动摩擦系数、丸粒化水稻种子-丸粒化水稻种子滚动摩擦系数及丸粒化水稻种子-PLA 板静摩擦系数分别为 0.137、0.137、0.336), 该研究能够为丸粒化种子的仿真参数标定及高速精量播种研究提供参考。

### INTRODUCTION

Rice is one of the most vital food crops globally and serves as a crucial source of sustenance for over half of the world's population (Djavan. et al., 2025). It is not only a staple in many countries but is also used in a variety of recreational dishes (Ning, 2016).

Rice planting represents a crucial aspect of rice production, with the planting technology exerting a direct influence on yield (Cai. et al., 2023). Currently, three methods of mechanical planting are in use: potting transplanting, mechanical transplanting, and mechanized direct seeding. The first two of these require seedling transplanting, a relatively complex process that results in higher overall production costs for seedling transplanting (Xue et al., 2022). The mechanized direct seeding of rice has the potential to streamline the planting process, and it has gained significant traction in numerous countries and regions in recent years. The majority of existing rice direct seeding techniques employ the use of tractor-tractor seeders and drones. The method of tractor-tractor seeders is still primarily limited to strip seeding, with precision seeding also facing significant challenges, particularly in the precise separation of rice seeds from the population. Additionally, the use of ground machinery has been observed to have relatively low efficiency. While existing unmanned aircraft seeding is highly efficient, it remains primarily a sowing method with several limitations. These include the disorderly arrangement of seeds on the ground and the difficulty of rapidly and precisely separating them from the population. The unique physical characteristics of rice, including high flow resistance and adhesion, present a significant challenge to the rapid and precise separation of seeds from the population, which has been a key obstacle to the development of high-speed precision rice planting.

<sup>1)</sup> Qianshu MA, master degree; Tongjie LI, Prof. Dr. Master's Degree Tutor; Donghan XU, master degree; Qingqing WANG\*, Dr, Lecturer.

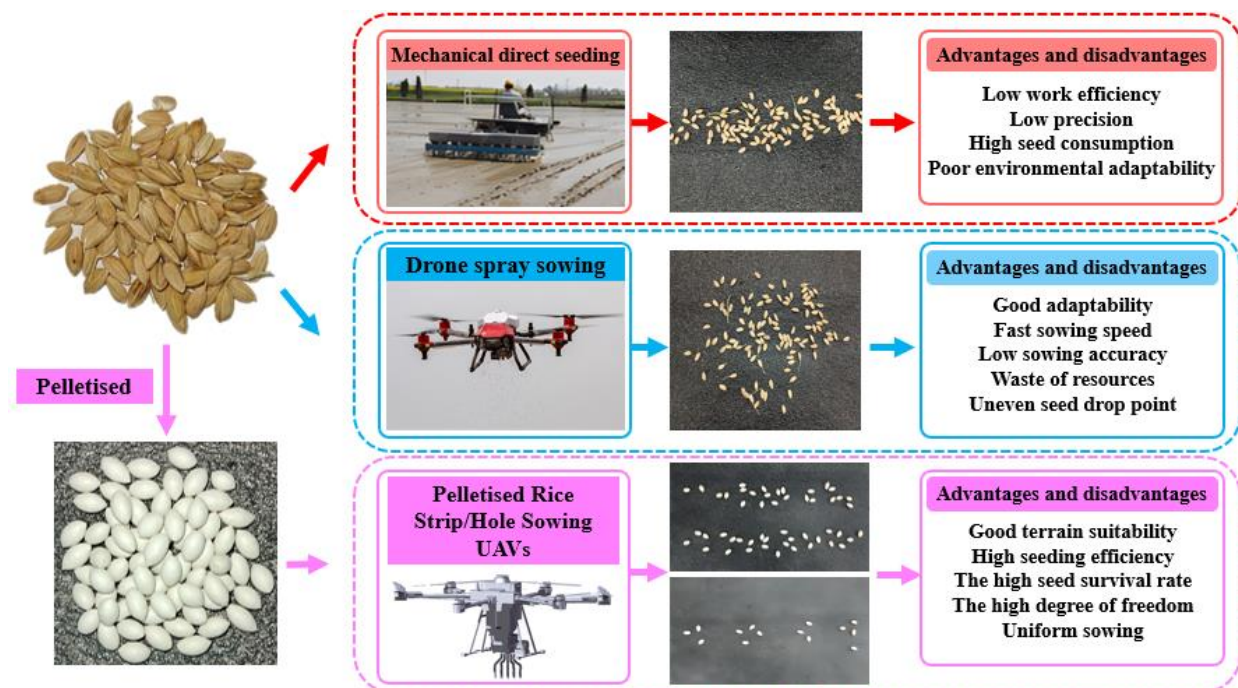


Fig. 1 - Comparison of direct seeding methods for rice

In light of the aforementioned considerations, our team proposed a method of pelleted rice seeds (PR), which can effectively solve the problem of rapid precision separation from the seed population, thus improving the sowing accuracy and sowing efficiency to carry out the subsequent high-speed precision planting of rice, as shown in Fig. 1, in the light of the characteristics of the physical structure of rice and planting needs. Seed pelleting treatment have been used in applications where germination, seedling emergence, resistance, and resistance to pests and diseases are improved (Ma et al., 2023; Yang et al., 2020; Wang et al., 2024). During the sowing process of PR, the forces between seeds and seeds and seeds and seed discharger are more complicated, and the parameter calibration of PRs can be carried out to find out their physical properties and promote the optimal design of pelleted seed discharger for precision hole sowing.

To date, researchers in both domestic and international settings have conducted simulations to calibrate discrete metamodells about fertilizers, soils, seeds, and crops. In a previous study, Wen Xiangyu et al. (2020) proposed a friction factor calibration method based on the overall characteristics of granular materials. This method was then used to calibrate the discrete meta-simulation parameters between urea particles and PVC materials. This calibration was carried out according to the results of the analysis of variance (ANOVA) of different particle characteristics testing methods. In a further contribution to this field of study, Wang Xianliang et al. (2021) employed the Edinburgh Elasto-Plastic Adhesion nonlinear elastic-plastic contact model to calibrate the parameters of a discrete element simulation model of perennial no-tillage agricultural soil. Balevičius et al. (2011) conducted a sliding test to measure the static coefficient of friction between peas and Plexiglas. González-Montellano et al. (2012) investigated direct measurement methods for some parameters in discrete element simulation. Xuejie Ma et al. (2022) calibrated the contact parameters of alfalfa seed and coating powder as the main research objects and carried out the related discrete element simulation parameter calibration. Peng Zhang et al. (2022) simulated and determined the contact parameters such as stacking angle, collision recovery coefficient, static friction factor, etc., using Xinjiang cotton straw as the test material. As evidenced by the aforementioned research, the majority of discrete element simulation parameters have been calibrated for large seeds and soil. However, there is a lack of research on the calibration of discrete element simulation parameters for PR and other pelleted crop seeds.

In this paper, the discrete element simulation model of PR was calibrated and validated by combining physical tests with discrete element simulation. The angle of repose was used as the response variable. Furthermore, the Plackett-Burman test, the steepest-climbing test, and the Box-Behnken test were conducted sequentially. A two-sample t-test was conducted on the simulation results and experimental data using SPSS 23 software to ascertain the reliability of the simulation tests and identify the optimal combination of simulation parameters. This study serves as a reference for developing high-speed precision seeding of granular seeds, which aids in optimizing both the seeding equipment and the seed treatment process.

## MATERIALS AND METHODS

### Calibration of test materials and physical parameters

This paper is based on the study of early and mid-grain rice grown in large areas in southern and northern China. Hui Liangyu silk seed was used as an experimental subject to determine the external dimensions, thousand kernel weight, Poisson's ratio, and other basic physical properties of PR.

The PR exhibited an ellipsoidal shape, a compact texture, and a smooth surface. These characteristics could enhance the mobility and population separability of the seeds, as illustrated in Fig. 2. A total of 1,000 pill-PR were randomly selected and weighed using an electronic scale with an accuracy of 0.01 g to determine the thousand-grain weight. The seeds were divided into 10 groups and weighed separately, and the average value was calculated. The thousand-grain weight of the pill-PR was found to be 134.05 g. The external dimensions of the pill-PR were measured using a numerical vernier caliper (with an accuracy of 0.01 mm), as illustrated in Fig. 2. The mean diameter ( $D$ ) and length ( $L$ ) of the seeds were found to be 5.17mm $\times$ 9.71mm, according to the measurement results.

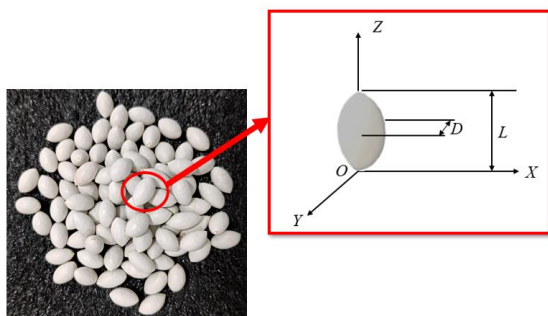


Fig.2 - Characteristic dimensions of PR



Fig.3 - Pressure deformation test of PR

One hundred PR were randomly selected and their original dimensions in radial ( $X$ -axis) and axial ( $Z$ -axis) directions were recorded. The compression deformation test of the PR was carried out using a universal material testing machine (UTM2501/50N, Shenzhen Sanshi Zongheng Technology), as shown in Fig. 3, with a test speed of 0.1 mm/min until the surface of the PR just broke (*Dun et al., 2024*). The radial deformation of the PR before and after the test was obtained using a universal material testing machine, and then the axial deformation of the PR was measured using electronic calipers (accuracy of 0.01 mm), and the Poisson's ratio of the PR was calculated to take the average value of 0.42.

A total of one hundred PR were randomly selected and their original dimensions in the radial ( $X$ -axis) and axial ( $Z$ -axis) directions were recorded. A universal material testing machine (UTM2501/50N, Shenzhen Sanshi Zongheng Technology) was employed to conduct pressure deformation tests on PR at a rate of 0.1 mm/min until the surface of the PR reached the point of rupture (*Dun et al., 2024*). The radial deformation of the PR was obtained using a universal material testing machine before and after the test. The axial deformation of the PR was then measured by electronic vernier calipers (accuracy of 0.01 mm), and the Poisson's ratio of the PR was calculated to yield an average value of 0.42.

### Determination of exposure parameters

The contact parameters are primarily comprised of the static friction coefficient, rolling friction coefficient, collision recovery coefficient, and stacking angle (*Hou et al., 2020*). The contact parameters between the PR and the contact materials, as well as between the seeds themselves, represent crucial design parameters for a seed discharge device. In light of the engineering practice and the manufacturing materials of the seed discharger (*Xing et al., 2020*), this paper selects the contact parameters between the steel plate, the PLA material, and the PR, as well as the contact parameters between the PR.

### Static Friction Coefficient Measurement Test

In this experiment, the static friction coefficients of PR were measured using the oblique method (*Cong, 2014*), which involved the use of steel plates and PLA plates. The coefficients were determined by observing the forces acting between the seeds, pellets, and plates. The test was conducted on a custom-built apparatus, and the dimensions ( $L \times W \times H$ ) of the steel plate utilized for testing were 300mm $\times$ 300mm $\times$ 1mm, while the dimensions ( $L \times W \times H$ ) of the PLA plate were 200mm $\times$ 150mm $\times$ 10mm, as illustrated in Fig. 4. The measurement will be taken along the long axis of the plate to be tested. The inclination angle of the plate will be increased

gradually until the PR begins to slide down its surface. This angle, which represents the sliding friction angle  $\theta$ , will be recorded. Ten randomly selected PR seeds underwent three repetitions of the test to determine the tangent value of the sliding friction angle. This method was adopted to determine the static friction coefficient of the PR. The mean value of the static friction coefficient between the PR and the steel plate was 0.32, while the mean value of the static friction coefficient between the PR and the PLA plate was 0.34. To determine the coefficient of static friction between PR, the seeds were affixed to the PLA plate with tape, as illustrated in Fig. 4c. The resulting average value of the static friction coefficient between PR was 0.5.



Fig.4(a) - Test rig for coefficient of static friction between PR and steel plate



Fig.4(b) - Test rig for coefficient of static friction between PR and PLA plates



Fig. 4(c) - Test rig for inter-seed static friction coefficient of PR

### Rolling Friction Coefficient Measurement Test

In this study, the side slope test method, as described by *Dun et al.*, (2024), was employed for the measurement of the variables under investigation. The underlying test principle is illustrated in Fig. 5. The apparatus comprises a PLA plate with a known inclination angle and a horizontal PLA plate. To conduct the rolling friction coefficient test between PR and the PLA plate, the PR is positioned on the inclined PLA plate, with an inclined rolling length of 30 mm. This allows the seeds to roll naturally under the influence of gravity, and the rolling distance of the seeds is then measured on the horizontal PLA plate. The rolling distance between the PR and the PLA plate is derived from the formula (1). The rolling friction coefficient between the PR and the PLA plate was determined through a series of 10 repetitions (*Wen et al.*, 2020). The resulting mean value was calculated to be 0.14.

$$mg \sin \theta \times h_0 = \mu_0 mg \cos \theta \times h_0 + \mu_0 mgh_1 \quad (1)$$

where:

$m$  is the mass of PR, [Kg];  $\theta$  is the PLA plate tilt angle, [°];  $h_0$  is the rolling length of PR on an inclined PLA plate, [mm];  $\mu_0$  is the coefficient of rolling friction between PR and PLA plates;  $h_1$  is the rolling length of PR on a horizontal PLA plate, [mm].

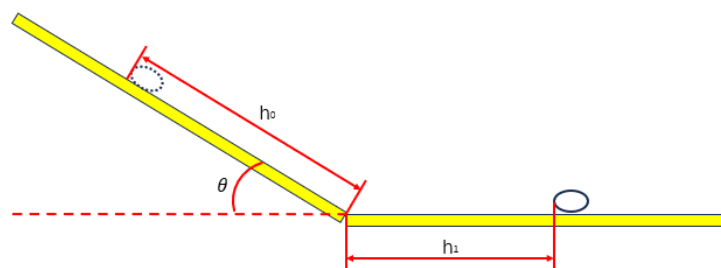


Fig.5 - Schematic diagram of side slope test

Replace the PLA plate in the above device with a steel plate, repeat the above test, and refer to the relevant literature (*Fan et al.*, 2024) to determine the rolling friction coefficient between the PR and the steel plate is 0.15.

In determining the rolling coefficient of friction between PR seeds, adhesive tape was used to uniformly fix the PR seeds onto two PLA boards. To account for the increase in rolling friction coefficient between the seeds, the angle of the inclined seed board was adjusted so that the sloping rolling length remained 30 mm. The above test was repeated 10 times, and following the relevant literature (*Wen et al.*, 2020), the average rolling coefficient of friction between PR seeds was determined to be 0.14.

### Crash recovery factor

Mutual extrusion and collision are expected to occur between PR seeds and the seed discharger during the seed discharge process. To quantify this phenomenon, the interspecies collision recovery coefficient must be calculated (Hou *et al.*, 2020). This coefficient is defined as the ratio of the relative velocity of separation of two objects after a collision to their relative approach velocity before the collision. It is calculated using Equation (2) (Dun *et al.*, 2024). The collision recovery coefficient was determined through a free-fall test, the methodology of which is illustrated in Fig. 6. The distance between the funnel of the test bench and the PLA plate was set to 100 mm. The background plate had a spacing of 10 mm per frame, and a digital camera was used for high-speed photography, with the video slowed down by a factor of 10. The rebound height was measured after the seeds made contact with the PLA plate. Each set of data was tested 10 times, and the average value was calculated. The results yielded a collision recovery coefficient of 0.298 between PR and the PLA plate, 0.279 for interspecies collisions of PR, and 0.320 between PR and the non-steel plate.

$$e = \frac{|v_2 - v_1|}{|V_2 - V_1|} = \frac{|v_2|}{|V_2|} = \sqrt{\frac{h}{H}} \quad (2)$$

where:

$V_1$  is the initial velocity of the PR in free fall, i.e.  $V_1 = 0 \text{ m/s}$ ;  $V_2$  is the initial velocity of the PR before it touches the PLA plate, [m/s];  $v_1$  is the velocity of the PR when it bounces up at the highest point after colliding with the PLA plate, [m/s];  $v_2$  is the velocity of the PR after colliding with the PLA plate, i.e.  $v_2 = 0 \text{ m/s}$ ;  $h$  is the height of the PR before free fall, [mm];  $H$  is the highest height at which the PR bounces back from the free-fall collision with the PLA plate, [mm].

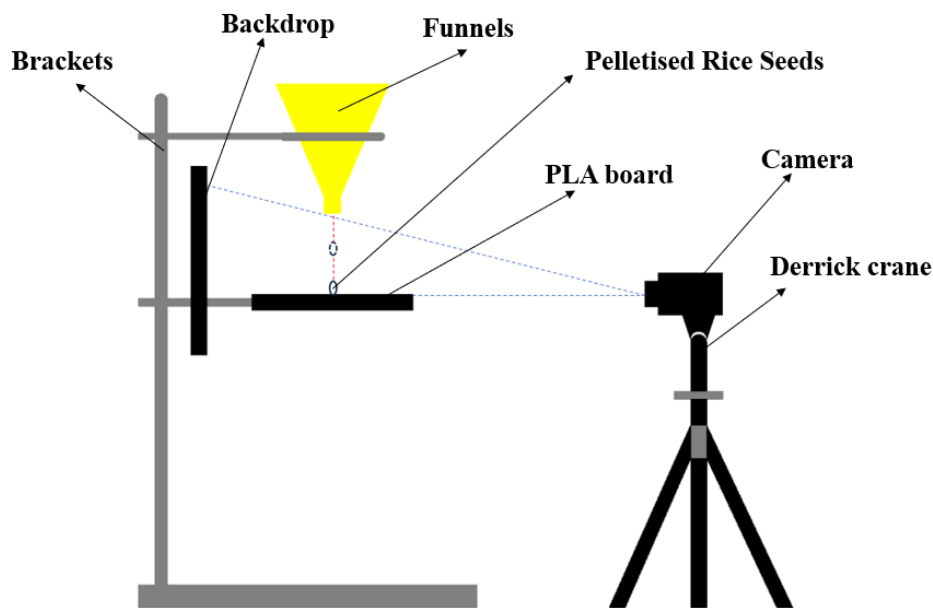


Fig. 6 - Schematic diagram of free fall test for PR

### Stacking angle

The stacking angle is a macroscopic parameter that reflects the fluidity and friction characteristics of granular materials. Additionally, a seed stacking process occurs during the sowing of PR. To further verify the accuracy of the calibration parameters, the stacking angle was selected as a test index. In this experiment, the stacking angle was measured using the funnel method, as previously described in detail by Zhu *et al.*, (2022) and Al-Hashemi B.M.H. *et al.*, (2018). The test is shown in Fig. 7(a). The PR is placed into the funnel, where it falls into a pile on the PLA platform. The centerline of the camera is set to the same height as the PLA platform. Images of the PR stacking are captured using image processing software to measure the stacking angle, as illustrated in Fig. 7(b). This process is repeated 10 times to obtain an average angle, which represents the pill-PR stacking angle.

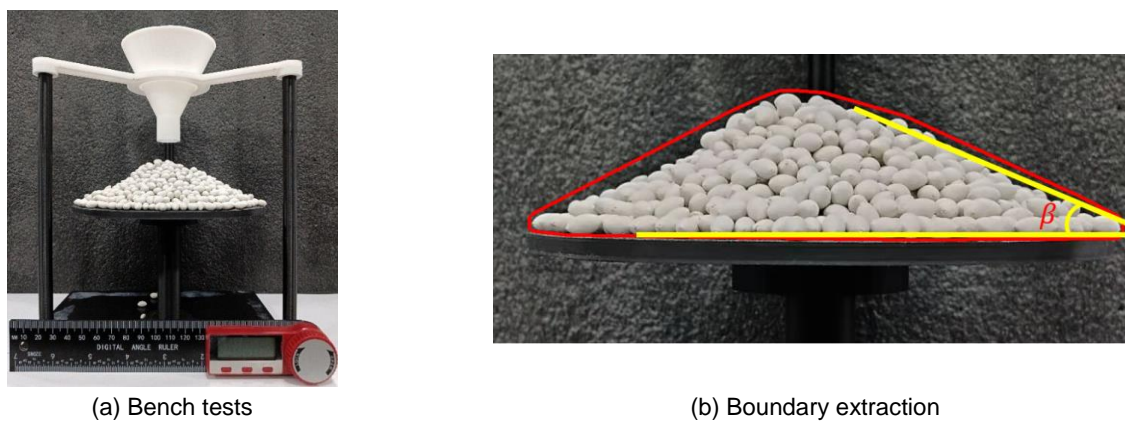


Fig. 7 - PR stacking angle test

### **Discrete elemental modeling of PR and calibration of simulation parameters**

#### **Development of a discrete meta-simulation model for PR**

The external dimensions of the PR were determined through preliminary physical testing. Based on the test data obtained, the average dimensional values for each axis were calculated and then modeled using SolidWorks software. The generated models were saved in STL format and subsequently imported into EDEM software. As demonstrated in the related literature (Zhang *et al.*, 2017), the simulation modeling process is most significantly affected by the interaction between PR-PR, and PR-PLA plates, as well as the size and shape of the simulation model. The contour of the model, the rounded corners of the edges filled with PR, and the PR filled with spherical particles via EDEM software had minimal effect on the simulation results.

In the EDEM simulation test, the data obtained from the aforementioned test were inputted, and the stacking angle determination model was drawn according to the size of the actual stacking angle determination device, as illustrated in Fig. 8. A particle factory was constructed at the large aperture above the funnel for the dynamic generation of PR. The PR was generated in a fixed form (Hou *et al.*, 2020), with a generation rate of 1000 particles/s and a total of 600 particles. The grid size was three times the minimum particle radius (Hu, 2010). At the outset of the simulation, the PR was generated from the pellet plant situated above the funnel and subsequently descended under the influence of gravity. The seeds were generated in a continuous stream over 0.6 seconds, after which the simulation concluded at 2 seconds. The seeds coalesced into a seed pile on the chassis, and the stacking angle was subsequently determined through post-processing of the seed pile.

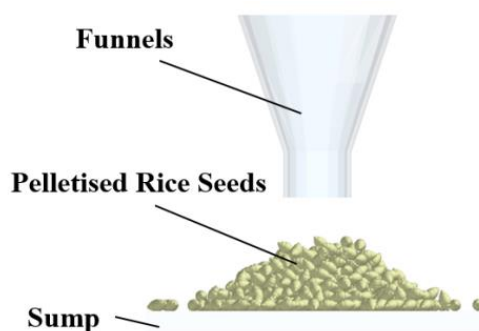


Fig. 8 - A simulation model for determining the stacking angle of PR

#### **Discrete element simulation parameter calibration**

##### **Determination of the significant impact factor**

The Design-Expert software was used in this study for the design of the Plackett-Burman experiment and data analysis. Plackett-Burman is a two-level design of experiments method that identifies significant parameters by comparing the difference between two levels of each parameter to the overall difference to determine the significance of the parameter (Bai *et al.*, 2023). The experimental parameters were identified based on the results of the physical tests described earlier. Parameters that had a significant effect on the response values were identified using the Plackett-Burman test (Li *et al.*, 2020). The maximum and minimum values of the seven test parameters listed in Table 1 were assigned +1 and -1, respectively. The Plackett-Burman test protocol and results are listed in Table 2.

Table 1

**Plackett-Burman test parameter range table**

Test parameters	Low level(-1)	High level(+1)
Poisson's ratio of PR (x1)	0.3	0.5
Rolling friction coefficient of PR-PLA plate (x2)	0.1	0.2
PR - Rolling Friction Coefficient of PR (x3)	0.1	0.2
Coefficient of static friction of PR-PLA plate (x4)	0.3	0.4
PR - Coefficient of static friction of PR (x5)	0.4	0.6
PR-PLA plate collision recovery coefficient (x6)	0.2	0.4
PR - Collision Recovery Coefficient of PR (x7)	0.2	0.4

Table 2

**Plackett-Burman test program and results**

Serial number	Test parameters							Stacking angle
	x1	x2	x3	x4	x5	x6	x7	
1	1	1	-1	1	1	1	-1	24.65
2	-1	1	1	-1	1	1	1	28.48
3	1	-1	1	1	-1	1	1	28.03
4	-1	1	-1	1	1	-1	1	25.77
5	-1	-1	1	-1	1	1	-1	23.31
6	-1	-1	-1	1	-1	1	1	17.63
7	1	-1	-1	-1	1	-1	1	18.10
8	1	1	-1	-1	-1	1	-1	19.05
9	1	1	1	-1	-1	-1	1	24.45
10	-1	1	1	1	-1	-1	-1	33.95
11	1	-1	1	1	1	-1	-1	34.61
12	-1	-1	-1	-1	-1	-1	-1	16.72

The data were imported into Design-Expert 13.0 software for analysis of variance (ANOVA) of the experimental results to determine the effect of each parameter. From the analysis, it was found that the coefficient of rolling friction of PR-PLA plate (X2), the coefficient of rolling friction of PR-PLA plate (X3) and the coefficient of static friction of PR-PLA plate (X4) had a significant effect on the stacking angle of PR, with P-values of 0.0726, 0.0024, and 0.0096, respectively. These values indicate a significant impact on the stacking angle, while the remaining parameters had relatively minor effects. Therefore, only the above three factors with significant effects were considered in the subsequent steepest climb test and Box-Behnken test.

**Steepest climb test design**

Based on the results of the Plackett-Burman test, the steepest climb test was conducted for the three selected significance factors (coefficient of rolling friction of PR-PLA plate, coefficient of rolling friction of PR-PLA seed, and coefficient of static friction of PR-PLA plate), and the relative error between the simulated stacking angle and the actual stacking angle was taken as the evaluation index to determine the optimum ranges of the above three test parameters (Liu et al., 2020). The design scheme and results of the steepest climb test are shown in Table 3.

For the simulation tests, all other insignificant parameters from the theoretical test results mentioned above were used: the PR Poisson's ratio 0.42, the PR-PR static friction coefficient 0.5, the PR-PLA plate collision recovery coefficient 0.298, and the PR-PR collision recovery coefficient 0.279.

Table 3

Steepest Climbing Test Design Options and Results

Serial number	x2	x3	x4	Stacking angle (°)	Relative error/%
1	0.1	0.1	0.3	15.82	0.323642582
2	0.12	0.12	0.32	20.22	0.135528003
3	0.14	0.14	0.34	25.3	0.081658829
4	0.16	0.16	0.36	27.24	0.164600257
5	0.18	0.18	0.38	29.24	0.250106883

According to the relative error results in Table 4, it can be seen that the rolling friction coefficient of PR and PLA plate and PR are both 0.14, and the static friction coefficient of PR-PLA plate is 0.34, the relative error between the simulated stacking angle and the actual stacking angle is small. It can be determined that the range of optimal intervals is in the vicinity of No. 3. Therefore, the follow-up will take No. 3 as the center point, and No. 2 and No. 4 as the low, high levels for subsequent Box-Behnken response surface tests.

**Box-Behnken experimental design**

In this paper, the Box-Behnken test design was performed using Design-Expert 13.0 software. This method fits a functional relationship between the parameters and response values to determine the interactions among the parameters. The solver is used to find the optimal values of the significant parameters (Bai et al., 2023). The Box-Behnken test for significance parameters was performed with No. 3 as the center point, No. 2 and No. 4 as the low (-1) and high (+1) levels, and all other parameters in the simulation test were set according to the parameters used in the steepest climb test. The test scheme and results are shown in Table 4.

Table 4

Box-Behnken experimental design scheme and results

Serial number	x2	x3	x4	Stacking angle (°)
1	-1	-1	0	23.77
2	1	-1	0	25.88
3	-1	1	0	25.54
4	1	1	0	27.62
5	-1	0	-1	24.81
6	1	0	-1	22.84
7	-1	0	1	23.45
8	1	0	1	26.71
9	0	-1	-1	24.98
10	0	1	-1	27.18
11	0	-1	1	26.89
12	0	1	1	27.16
13	0	0	0	23.57
14	0	0	0	23.15
15	0	0	0	23.90

The above test results were analyzed and fitted with multiple regression using Design-Expert 13.0 software to obtain the following second-order regression equations for the stacking angle of the PR simulation test:

$$\beta = 23.54 + 0.56A + 0.5675B + 0.575C - 0.2575AB + 1.31AC - 0.4325BC - 0.0687A^2 + 1.98B^2 + 0.9812C^2 \tag{3}$$

**RESULTS**

The results of Box-Behnken test ANOVA are shown in Table 5. From the analysis of the results in Table 5, it can be observed that factors A (x1), B (x2), C (x3), AC, B2, and C2 have a significant effect on the stacking angle, while the effect of AB, BC, A2 on the stacking angle is not significant. The p-value of this fitted model is 0.0013 (p<0.01), which indicates the relationship between the dependent and independent variables and its significance in the model; the lack-of-fit term P=0.5003>0.05, suggests that the model is well fitted. The coefficient of determination for the second-order regression equation of the stacking angle R^2=0.9775 and the adjusted coefficient of determination is R^2=0.9371, both of which are very close to one. In general, the

higher the coefficient of variation (CV), the lower the reliability of the test, In this test, the CV=1.56% which indicates that the fitted equation has a high degree of credibility and accurately represents real conditions, thereby verifying the test's reliability.

Table 5

Box-Behnken design Second order regression equation Analysis of variance

Source	Sum of squares	df	Mean Square	P-value
<b>Model</b>	33.2	9	3.69	0.0013
A (x1)	2.51	1	2.51	0.0098
B (x2)	2.86	1	2.86	0.0075
C (x3)	2.64	1	2.64	0.0088
AB	0.2652	1	0.2652	0.2446
AC	6.84	1	6.84	0.0011
BC	0.7482	1	0.7482	0.0777
A <sup>2</sup>	0.0175	1	0.0175	0.749
B <sup>2</sup>	14.49	1	14.49	0.0002
C <sup>2</sup>	3.56	1	3.56	0.0048
<b>Residual</b>	0.7631	5	0.1526	
<b>Lack of fit</b>	0.4805	3	0.1602	0.5003
<b>Pure Error</b>	0.2826	2	0.1413	
<b>Cor Total</b>	33.96	14		
<i>R<sup>2</sup> = 0.9775; Adjusted R<sup>2</sup> = 0.9371; CV = 1.56%</i>				

In the data analysis optimization module of Design-Expert 13.0 software, the second-order regression equations were refined by averaging the results from 100 sets of optimal combinations. The coefficient of rolling friction between PR and PLA plates was found to be 0.137, reflecting the interaction of the PR on the surface of the PLA plate as well as among the seeds themselves. Meanwhile, the coefficient of static friction for the PR against the PLA plate was measured at 0.336, indicating the maximum frictional force encountered when the PR remains relatively stationary before rolling. The remaining parameters, which were considered insignificant, were averaged based on physical tests. To validate the accuracy of these optimal parameter combinations, simulation tests were performed using EDEM, as depicted in Fig.9. The stacking angles recorded from three replicates were 24.15°, 23.97°, and 22.97°. A t-test analysis comparing the simulation results with the actual test values, conducted using SPSS 23 software, produced a p-value of 0.481, which exceeds the 0.05 threshold. In statistical terms, a p-value greater than 0.05 typically indicates no significant difference between the two data sets. Consequently, this result confirms that the outcomes of the simulation tests align closely with the real physical test values, further demonstrating the accuracy and reliability of the optimal parameter combination.

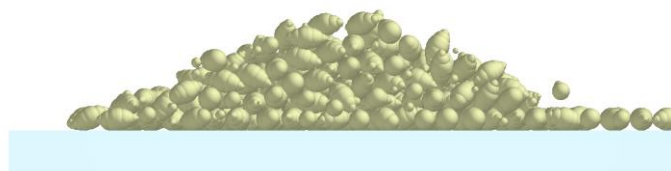


Fig. 9 - Validation of discrete element simulation of pile-up angle of PR

**CONCLUSIONS**

(1) The physical properties of the particulate material—including external dimensions, micrometric weight, and Poisson's ratio—along with the contact parameters, such as the static friction coefficient, rolling friction coefficient, and collision recovery coefficient, are established through physical testing. This process provides the essential parameters required for the discrete element simulation of the particle system.

(2) The Plackett-Burman test was performed according to the specified parameters to determine which factors most significantly affect the PR stack angle. The parameters under investigation include the rolling friction coefficient of the PR-PLA plate, the rolling friction coefficient of the PR-PR, and the static friction coefficient of the PR-PLA plate.

(3) The second-order regression equation for the stacking angle was derived using a Box-Behnken test. Following optimization and solving, the optimal simulation parameters identified are as follows: the rolling friction coefficient of the PR-PLA plate is 0.137, the rolling friction coefficient of the PR-PR plate is also 0.137, and the static friction coefficient of the PR-PLA plate is 0.336. Simulation experiments were conducted using these parameters, and a T-test analysis was performed to examine the correlation between the simulation results and the actual experimental values. The T-test analysis reveals no significant difference between the simulation results and the experimental values ( $P > 0.05$ ), further confirming the authenticity and reliability of the simulation parameters after the experiments and calibration.

(4) This conclusion not only serves as a reference for research on PR and their high-speed precision sowing but also provides valuable insights for the practical application of these seeds in agriculture. This information can help optimize the seeding equipment design and seed handling process at a later stage, thus improving the efficiency and quality of agricultural production.

## ACKNOWLEDGEMENTS

The authors would like to express their gratitude to the anonymous reviewers for their insightful comments. This research was funded by the Key Project of the Department of Education of Anhui Province (Grant No.2024AH050307), the Collaborative Innovation Project of Universities in Anhui Province (Grant No. GXXT-2023-042), and the Anhui University of Science and Technology Talent Introduction Project (Grant No. JXYJ202201).

## REFERENCES

- [1] Al-Hashemi B.M.H., Al-Amoudi B.S.O. (2018). A review of the angle of repose of granular materials. *Powder Technology*, Vol. 330, pp. 397-417. <https://doi.org/10.1016/j.powtec.2018.02.003>
- [2] Bai J.Y., Xie B., Yan J.G., Zheng Y., Liu N., Zhang Q., (2023) Moisture content characterization method of wet particles of brown rice based on discrete element simulation. *Powder Technol.* Vol. 428, pp. 118775. <https://doi.org/10.1016/j.powtec.2023.118775>.
- [3] Cai M.Y., Ren X.Z. (2023). Current status and development characteristics of rice mechanized planting technology (水稻机械化种植技术现状及发展特征). *Use and Maintenance of Agricultural Machinery*, Vol. 317(1), pp. 99-102. <https://doi.org/10.14031/j.cnki.njwx.2023.01.029>. (in Chinese)
- [4] Cong J.L. (2014). *Research on the Mechanism and System of Pneumatic Precision Seed Metering for Rapeseed and Wheat* (油菜小麦兼用型气力式精量排种系统及其机理研究). [Doctoral dissertation, Wuhan: Huazhong Agricultural University]
- [5] Djavan De Clercq; Adam Mahdi. (2025). Modern computational approaches for rice yield prediction: A systematic review of statistical and machine learning-based methods. *Computers and Electronics in Agriculture*, Vol. 231, pp. 109852-109852. <https://doi.org/10.1016/J.COMPAG.2024.109852>
- [6] Dun G.Q., Wang L., Ji X.X., Jiang X.Y., Zhao Y., Guo N. (2024). Calibration and experimental verification of discrete element parameters for Jinxing purple garlic seeds (金乡紫皮蒜种离散元参数标定与试验验证). *China Agricultural Science and Technology Review*, Vol. 26(8), pp. 131-139. <https://doi.org/10.13304/j.nykjdb.2022.1023>. (in Chinese)
- [7] Dun G.Q., Wang L., Ji X.X., Jiang X.Y., Zhao Y., Guo N. (2024). Calibration and experimental verification of discrete element simulation model parameters for radish seeds (c). *Journal of Agricultural Mechanization Research*, Vol. 45(9), pp. 127-133. <https://doi.org/10.13733/j.jcam.issn.2095-5553.2024.09.019>. (in Chinese)
- [8] Fan C.S., He R.Y., Shi Y.Y., Wang J.L., Xu G.M. (2024). Study on parameter calibration method for organic-inorganic mixed fertilizer using discrete element method (有机无机混合肥料离散元参数标定方法研究). *Journal of Nanjing Agricultural University*, Vol. 47(2), pp. 402-413. (in Chinese)
- [9] Ge T., Jia Z.H., Zhou K.D. (2007). A theoretical model for calculating the restitution coefficient of point-contact collisions (计算点接触碰撞恢复系数的一种理论模型). *Journal of Mechanical Design and Research*, Vol. 3, pp. 14-15+22. <https://doi.org/10.13952/j.cnki.jofmdr.2007.03.019>. (in Chinese)
- [10] González-Montellano C., Fuentes J.M., Ayuga-Téllez E., Ayuga F. (2012). Determination of the mechanical properties of maize grains and olives required for use in DEM simulations. *Journal of Food Engineering*, Vol. 111(4), pp. 553-562. <https://doi.org/10.1016/j.jfoodeng.2012.03.017>
- [11] Hou Z.F., Dai N.Z., Chen Z., Zhang X.W. (2020). Determination of physical parameters of *Elymus nutans* seeds and calibration of DEM simulation parameters (冰草种子物性参数测定与离散元仿真参数标定). *Transactions of the Chinese Society of Agricultural Engineering*, Vol. 36(24), pp. 46-54. (in Chinese)

- [12] Hu G.M. (2010). *Discrete Element Method Analysis and Simulation of Granular Systems: Introduction to Industrial Applications of Discrete Element Method and EDEM Software* (颗粒系统的离散元素法分析仿真: 离散元素法的工业应用与 EDEM 软件简介). Wuhan: Wuhan University of Technology Press. (in Chinese)
- [13] Liu H.Y., Lu Q., Wang J.W., Zhou W.Q., Wang N.H. (2024). Rapid calibration method for discrete element simulation parameters of columnar granular organic fertilizer with variable moisture content. *Powder Technology*, Vol. 448 pp. 120354. <https://doi.org/10.1016/J.POWTEC.2024.120354>
- [14] Liu F.Y., Zhang J., Li B., Chen J. (2016). Analysis and calibration of discrete element parameters of wheat based on bulk density test (基于堆积试验的小麦离散元参数分析及标定). *Transactions of the Chinese Society of Agricultural Engineering*, Vol. 32(12), pp. 247-253. (in Chinese)
- [15] Li H.Q., Zhang G.C., Li X.C., Zhang H.B., Zhang Q., Liu W.B., Mu G. (2021). Calibration of the discrete element method parameters in living juvenile Manila clam (*Ruditapes philippinarum*) and seeding verification. *AgriEngineering*, Vol. 3(4), pp. 894-906.
- [16] Ma X.J., Hou Z.F., Liu M. (2022). Calibration of simulation parameters of coated particles and analysis of experimental results. *INMATEH-Agricultural Engineering*, Vol. 67(2), pp. 233-242. <https://doi.org/10.35633/inmateh-67-23>
- [17] Ma Y., Wang X.L., Wang Y.L., Ma Y.T., Cui H.P. (2023). Research progress on seed pelleting in the field of ecological restoration (生态恢复领域草种丸粒化研究进展). *Chinese Journal of Grassland*, Vol. 32(4), pp. 197-207. (in Chinese)
- [18] Ning X. (2016). *Research on Environmental Adaptation of China's Major Grain Crop Cultivation under Climate Change* (气候变化下我国主要粮食作物种植环境适应性研究). [Doctoral dissertation, Henan University]
- [19] R. Balevičius; I. Sielamowicz; Z. Mróz; R. Kačianauskas. (2011). Investigation of wall stress and outflow rate in a flat-bottomed bin: A comparison of the DEM model results with the experimental measurements. *Powder Technology*, Vol. 214(3), pp. 322-336. <https://doi.org/10.1016/j.powtec.2011.08.042>
- [20] Wang X.L., Zhong X.K., Geng Y.L., Wei Z.C., Hu H., Geng D.Y., Zhang X.C. (2021). Calibration of no-tillage soil parameters based on nonlinear elastic-plastic contact model in DEM (基于离散元非线性弹塑性接触模型的免耕土壤参数标定). *Transactions of the Chinese Society of Agricultural Engineering*, Vol. 37(23), pp. 100-107. (in Chinese)
- [21] Wang X.Q., Pi N.N., Weng Q.F. (2024). Seed pelleting and its research progress (种子丸粒化及其研究进展). *Hunan Agricultural Science*, Vol. 3, pp. 85-90. <https://doi.org/10.16498/j.cnki.hnnykx.2024.003.018>. (in Chinese)
- [22] Wen X.Y., Yuan H.F., Wang G., Jia H.L. (2020). Study on calibration method for friction coefficient in discrete element simulation of granular fertilizer (颗粒肥料离散元仿真摩擦因数标定方法研究). *Transactions of the Chinese Society for Agricultural Machinery*, Vol. 51(2), pp. 115-122+142. (in Chinese)
- [23] Xing X.P., Ma X., Chen L.T., Li H.W., Wen Z.C., Zeng G.Z. (2020). Experimental study on physical properties of solid granular fertilizers (固体颗粒肥料物理特性的试验研究). *Research on Agricultural Mechanization*, Vol. 42(9), pp. 125-130. <https://doi.org/10.13427/j.cnki.njyi.2020.09.022>. (in Chinese)
- [24] Xue K., Gao K., Kuang F., Zhang S., Liao J., Zhu D. (2022). Machinery-plant-paddy soil coupling model based numerical simulation method of mechanical transplanting process of big rice seedling. *Computers and Electronics in Agriculture*, vol.198, <https://doi.org/10.1016/J.COMPAG.2022.107053> (in Chinese)
- [25] Yang M.X., Zhang Y., Han L.P. (2020). Screening of pelleting formula for sorghum-sudangrass hybrid seeds (高丹草种子丸粒化配方的筛选). *Henan Agricultural Science*, Vol. 49(7), pp. 58-67. <https://doi.org/10.15933/j.cnki.1004-3268.2020.07.008> (in Chinese)
- [26] Zhang R., Han D.L., Ji Q.L., He Y., Li J.Q. (2017). Study on parameter calibration method of sand in discrete element simulation (离散元模拟中沙土参数标定方法研究). *Transactions of the Chinese Society for Agricultural Machinery*, Vol. 48(3), pp. 49-56. (in Chinese)
- [27] Zhang P., Zhang H., Li J., Tan C., Zhang J. (2022). Parametric calibration of cotton straw parameters in Xinjiang based on discrete elements. *INMATEH - Agricultural Engineering*, Vol. 67(2), pp. 314-322. <https://doi.org/10.35633/inmateh-67-32>
- [28] Zhu X.H., Fu S.K., Li X.D., Wei Y.Q., Zhao W. (2022). Research on general calibration method of discrete element parameters for sheep manure with different moisture contents (不同含水率羊粪离散元参数通用标定方法研究). *Transactions of the Chinese Society for Agricultural Machinery*, Vol. 53(8), pp. 34-41. (in Chinese)